

Fracture energy of UHP-FRC under direct tensile loading

K. Wille & A. E. Naaman

University of Michigan, Ann Arbor, USA

ABSTRACT: A research was conducted to investigate and improve the fracture energy of ultra high performance fiber reinforced concretes (UHP-FRC) using relatively low fiber contents. Seven different UHP-FRCs incorporating different types and amounts of high strength steel fibers were tested in tension, using double-bell shaped tensile prisms. The UHP-FRCs were first optimized to achieve a compressive strength of about 200 MPa, without applying any heat curing treatment or pressure. The high strength steel fibers used were smooth, hooked-ends or twisted. Particular attention was placed to measuring the strain-hardening and softening performance of the composite in order to accurately evaluate the dissipated energy per unit area and per unit volume. An optimized UHP-FRC with 1.5 % twisted steel fibers by volume exceeded 30 kJ/m^2 in fracture energy. This is about one and a half the fracture energy reported from other comparable UHP-FRC.

1 INTRODUCTION

Ultra high performance concretes (UHPC) are characterized by a very high packing density. This leads to ultra high compressive strength, which results in an explosive failure in compression, and a very brittle failure in tension. One solution to overcome this brittle behavior is to add fibers to the concrete. When the fiber and matrix parameters are properly selected, the addition of fibers can improve the fracture energy G_f of such ultra high performance fiber reinforced concretes (UHP-FRC) by several orders of magnitude, thus arousing significant interest for practical applications. The fracture energy is influenced by numerous variables which include the fiber and matrix properties, their bond behavior, and the average number and inclination of fibers crossing the crack. Assuming steel fibers with high strength and ductility are used, the fracture energy of UHPC can be enhanced 1) by improving the physico-chemical bond through higher matrix strength and packing density, 2) by improving the mechanical bond through deformed steel fibers, and 3) by increasing the amount of fibers. However, the amount of fibers is limited by the workability of the composite. A low workability may lead to air entrapment and decreased compressive strength. Therefore, there is a need to optimize various parameters in order to maximize the fracture energy of the composite in tension. In this study a limit on the fiber volume fraction was set at 2.5 % to maximize the benefits to cost ratio. Since compressive failure is induced by splitting tensile cracks in the concrete, the addition of fibers is therefore expected to quell the explosive nature of compression failure of UHPC.

2 BACKGROUND INFORMATION

2.1 Strain hardening

If the stress σ_{cc} is defined as the applied tensile load, when the first precolation crack occurs, divided by the specimen cross sectional area A , and if the maximum post-cracking stress σ_{pc} is defined as the maximum tensile load divided by the specimen cross sectional area A , Equation 1 can be formulated to define "high performance FRC" which in effect implied strain hardening behavior. An account of the history and evolution of the terminology leading to strain-hardening is given by Naaman (2007).

$$\sigma_{pc} \geq \sigma_{cc} \quad (1)$$

Figure 1a illustrates a simplified response of strain-hardening fiber reinforced concrete comprising three conceptual parts, Part I (Elastic behavior up to 90-95% of σ_{cc} , followed by development of micro cracks and activation of fibers), Part II (Strain hardening behavior with multiple cracking, small crack width, providing inelastic strain) and Part III (Softening behavior with opening of a major crack).

All seven UHPFRC investigated in this study exhibited strain hardening behavior (Fig. 2).

2.2 Fracture Energy

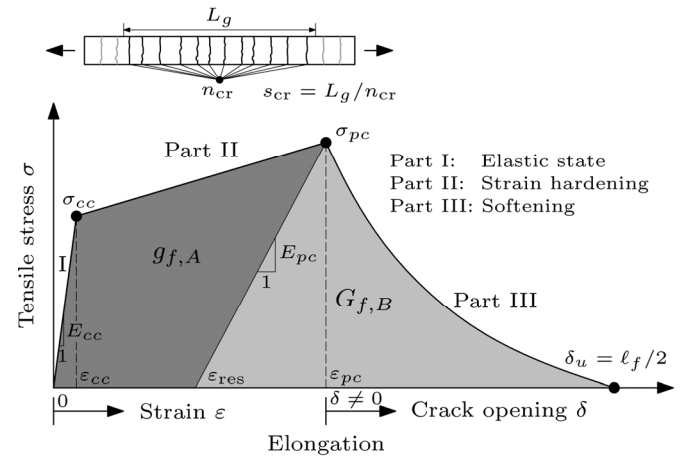
Fracture energy G_f is defined as the amount of dissipated work W needed to generate a unit crack with two completely separated crack surfaces ($2 A_{Lig}$); if the new crack area or fracture area, or ligament area is defined as A_{Lig} then:

$$G_f = \frac{W}{A_{Lig}} = \frac{\int_{\delta=0}^{\delta_u} F(\delta) d\delta}{A_{Lig}} \quad (2)$$

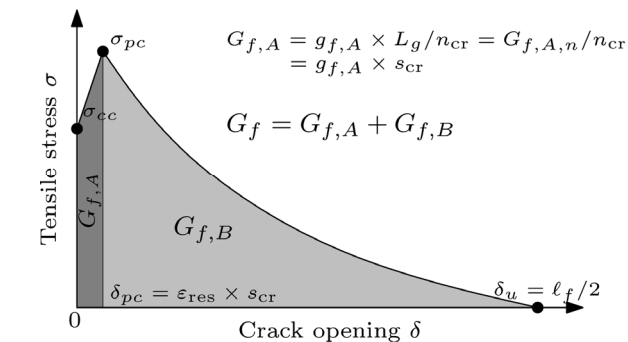
where F = load applied in tension; δ = crack opening, and δ_u crack opening up to complete separation.

Reported fracture energy values of UHP-FRC or other high performance cementitious composites are: 20 kJ/m² (2.5 % steel fibers, Jungwirth 2006), 20 kJ/m² (6 % steel fibers, Benson & Karihaloo 2005), 24 kJ/m² (6 % steel fibers, Habel et al. 2006), 25 kJ/m² (12 % steel fibers, Bache 1992), 34 kJ/m² (4 % PE(Spectra)-fibers, Maalej et al. 1995), 40 kJ/m² (2.5 % steel fibers, 90°C thermal treatment, Richard & Cheyrezy 1995).

The evaluation of fracture energy of strain hardening fiber reinforced concrete un-notched specimens under direct tension requires the distinction between the energy dissipated during strain hardening $G_{f,A,n}$ and the energy dissipated during softening $G_{f,B}$ per unit ligament area (Fig. 1).



a) Definition of energy per unit volume g_f and per unit area G_f



b) Definition of G_f related to the failure causing crack

Figure 1. Strain hardening material under tension and the definition of fracture energy related parameters.

The energy per unit area $G_{f,A,n}$ dissipated during strain hardening depends on the gauge length L_g used in measuring strain, and represents the energy needed to generate n_{cr} cracks with a permanent crack

opening, δ_{pc} . The ratio L_g / n_{cr} defines the average crack spacing, s_{cr} , assuming that within L_g an evenly distributed crack pattern is generated for a given composite. Thus the relative fracture energy g_f per unit gauge length can be defined as described below. This type of energy per unit volume is only related to strain hardening materials and allows an objective comparison of the strain hardening performance of different composites (Fig. 1).



Figure 2. Distinctive fine multiple cracking upon strain hardening of UHP-FRC with only 1.5 % twisted high strength steel fibers.

Reaching the peak stress or post-cracking strength, σ_{pc} , initiates the crack opening of one major crack, defined as the critical failure crack, and leads to the softening behavior of the material. A determination of residual strain ϵ_{res} as well as stiffness at peak load E_{pc} is needed to calculate the energy $G_{f,B}$, which represents the energy per ligament area to separate the major crack starting from a residual crack opening of δ_{pc} . Therefore, the entire fracture energy G_f needed to completely separate the material is determined from the following equations:

$$g_{f,A} = \int_{\epsilon=0}^{\epsilon_{pc}} \sigma(\epsilon) d\epsilon - \frac{1}{2} \frac{\sigma_{pc}^2}{E_{pc}} \quad (3)$$

$$G_{f,A} = g_{f,A} \times L_g / n_{cr} = G_{f,A,n} / n_{cr} \quad (4)$$

$$G_{f,B} = \int_{\delta=\delta_{pc}}^{\delta_u} \sigma(\delta) d\delta \quad (5)$$

$$\delta_{pc} = \epsilon_{res} \times s_{cr} = \left(\epsilon_{pc} - \frac{\sigma_{pc}}{E_{pc}} \right) \times \frac{L_g}{n_{cr}} \quad (6)$$

$$G_f = G_{f,A} + G_{f,B} \quad (7)$$

Figure 1 and Equations 3-7 point out the distinction between the relative fracture energy $g_{f,A}$ during strain hardening and the fracture energy $G_{f,B}$ during softening. Since in order to determine the fracture energy $G_{f,B}$ the stiffness E_{pc} is needed, it has been determined from the experimental results of this study and reported later in Table 4. The stiffness was calculated from the following equation:

$$E_{pc} = \frac{\sigma_{pc}}{\varepsilon_{pc} - \varepsilon_{res}} = \frac{\sigma_{pc}}{k_{\varepsilon} \times \varepsilon_{pc}} \quad (8)$$

where k_{ε} is a parameter that can be determined depending on the type of fiber and composite.

3 MATERIAL AND TEST SETUP

3.1 UHPC and UHP-FRC

An ultra high performance concrete (UHPC) was developed by properly selecting material components available in the US and fine-tuning their proportions and their interaction in the fresh state using the flow cone table (Wille et al., in press). The UHPC achieved a compressive strength at 28 days of 192 MPa (28 ksi), obtained from prism shaped specimens with a slenderness of 2 (50x50x100 mm), with ground loaded surfaces and cured under normal laboratory conditions (water, 20°C). No heat treatment, no pressure or special mixer was used following the goal of a simply way to design an UHPC, which in addition exhibits self consolidating properties providing good workability. The mix proportion and mechanical properties of the plain UHPC can be found in Table 1.

Table 1. Mixtures for UHPC and UHPFRC.

Type	UHPC	UHP-FRC
	Proportions by weight	
Cement PC Type I	1.0	1.0
Silica Fume	0.25	0.25
Quartz Powder	0.25	0.25
Water	0.22	0.22
Superplasticizer	0.0054*	0.0054*
Fine sand A**	0.28	0.26
Fine sand B***	1.10	1.03
Steel fibers****	0.00	0.25*****
f'_c [prism] in MPa (28d)	192	201
f'_c [prism] in MPa (140d)	210	n/a
Large spread value in mm	910	835

*solid content, ** max. grain size 0.2 mm, *** max. grain size 0.8 mm, **** straight, $l_f/d_f=13\text{mm}/0.2\text{mm}$, ***** 2.5 % by volume

The addition of high strength steel fibers up to 2.5 % by volume did not diminish the self consolidating properties of the mixture. The compressive strength of the UHP-FRC exceeded 200 MPa after 28 days.

3.2 Steel Fibers

Four types of high strength ($f_t > 2000$ MPa) steel fibers were used in this study (Table 2). These included straight smooth steel (S-) fibers, commonly used so far in UHPC mixtures worldwide; the S- fibers are characterized by a small diameter and an appropriate length to diameter ratio (l_f/d_f) giving good workability and bond behavior (Fig. 3a).

The three other fibers were deformed fibers which provided mechanical bond in addition to the physico-chemical bond. They included a commercially available hooked (H-) fiber which develops its mechanical bond through a hook-shaped deformation at each end, and two twisted (T-) fibers which provided mechanical bond distributed along their entire length.

Table 2. Types of fibers used in the study.

	Form	Twists	d_f	l_f	l_f/d_f
	-	-	mm	mm	-
S	straight	0	0.20	13	65
H	hooked	0	0.38	30	79
T ₁	high twisted	16	0.30*	30	100
T ₂	low twisted	6-8	0.30*	30	100

*manufactured out of round wire with $d_f=0.30$ mm, shaped into prism $a/b=0.24/0.30$ mm

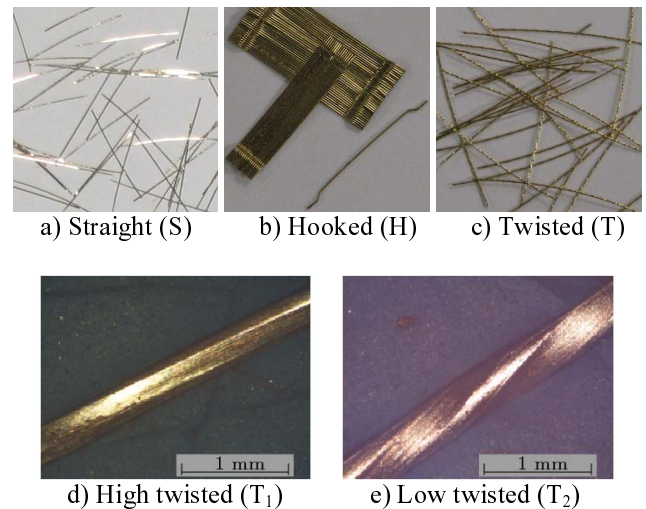


Figure 3. Different types of steel fibers used in this research.

The mechanical bond of the T- fiber is influenced by the number of twists and the torque resistance of the fiber. One T-fiber had a high twist ratio leading to about 16 ribs per fiber length, and the other had a lower twist ratio with about 6-8 ribs per fiber length, (Fig. 3e). Both T fibers were square in cross-section and were made from a wire with 0.3 mm in diameter.

3.3 Specimen Preparation

Cement (C), silica fume (SF), glass powder (GP), water, superplasticizer (SPL) and steel fibers were mixed together in a drum mixer following the rec-

ommended mixing procedure in (Wille et al. in press). After mixing, the UHP-FRC was poured in double-bell shaped tensile prisms; a slight vibration was applied at the end. After casting, the specimens were covered with plastic sheets and stored at room temperature for 24 hours. Then they were taken out of their molds and stored in a water tank at 20°C for an additional 25 days. All specimens were tested at the age of 28 days.

3.4 Test Setup

Double-bell shaped tensile prisms were loaded and unloaded under uniaxial tension (Fig. 4), following a displacement controlled procedure. Two symmetrically placed LVDTs were attached to the specimens over a gauge length L_g of 178 mm to measure the tensile elongation. The strain, valid up to peak stress, was obtained from the average elongation.

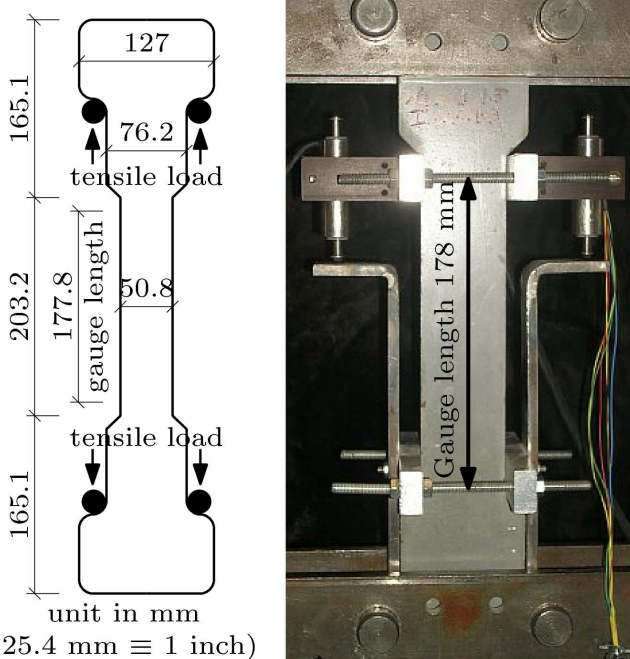


Figure 4. Shape of direct tensile specimen and test setup.

4 EXPERIMENTAL PROGRAM

An experimental program comprising seven series of UHP-FRC tensile tests was carried out (Table 3). An estimated lower limit for the fiber volume fraction to achieve strain hardening behavior was set to 1.5 % for S-fibers and 1.0 % for deformed fibers (H, T). This led to the first 3 series of tests. Moreover the volume fraction was increased by an additional 1 % leading to three additional series with 2.5 % of S-fibers and 2 % of H- and T-fibers. Following the goal to design a high ductility UHP-FRC with a low amount of fibers, a test series with 1.5 % of low twisted high strength steel fibers was also investigated (Table 3).

Table 3. Different types of UHP-FRC investigated in this study.

Notation	Form	Frac-tion V_f Vol.-%	Fiber Factor χ_f	
			$\chi_f = V_f \times l_f / d_f$	
UHP-FRC-S-1.5	S	1.5	1.2	≤ 2.5
UHP-FRC-S-2.5	S	2.5	2.0	≤ 2.5
UHP-FRC-H-1.0	H	1.0	0.8	≤ 2.0
UHP-FRC-H-2.0	H	2.0	1.6	≤ 2.0
UHP-FRC-T ₁ -1.0	T ₁	1.0	1.0	≤ 2.0
UHP-FRC-T ₁ -2.0	T ₁	2.0	2.0	≤ 2.0
UHP-FRC-T ₂ -1.5	T ₂	1.5	1.5	≤ 2.0

5 TEST RESULTS

5.1 Workability

It is generally accepted that, for a given fiber, the workability of FRC decreases with an increase in either the volume fraction of fibers or their aspect ratio. The product of volume fraction V_f by the aspect ratio l_f/d_f is often termed the fiber factor, χ_f , (Equation 9).

$$\chi_f = V_f \times l_f / d_f \quad (9)$$

Thus an increase in χ_f increases the risk of fiber clumping during the mixing process and decreases workability. Markovic (2006) recommended an upper limit of $\chi_f \approx 2.5$ (2006) considering straight fiber with $l_f/d_f = 13 / 0.2$ mm. For UHP-FRC with long fibers of $l_f/d_f = 30 / 0.3$ mm, the above limit suggests a maximum fiber volume fraction of 2.0 %.

5.2 Tensile Behavior under loading & unloading

Test results were analyzed for strain hardening performance and post-peak softening behavior, evaluated through the relative fracture energy $g_{f,A}$, and $G_{f,B}$, respectively. Particular attention was put to determine the stiffness E_{pc} at peak load since it is essential to distinguish the dissipated energy during strain hardening and softening.

The tensile responses of all UHP-FRC specimens tested are shown in Figure 5-11 and key properties are summarized in Table 4.

It can be observed first that all UHP-FRC specimens within each series showed a low variability in their tensile response. A volume fraction of 1.5 % of S-fibers can be considered a lower limit to obtain strain hardening behavior (crack spacing $s_{cr} \approx 25$ mm). A volume fraction of 1.0 % of H- or T-fibers was sufficient to clearly obtain strain hardening and multiple cracking (crack spacing $s_{cr} \approx 9$ mm). UHP-FRC-T₁-2.0 exhibited the highest tensile strength up to $\sigma_{pc} = 16$ MPa and the highest strain value at peak load, $\varepsilon_{pc} = 0.61$ %. With a final crack spacing $s_{cr} \approx 3$ mm and a residual average crack width of 7-8 microns (Fig. 12) this UHP-FRC

exhibited the best overall behavior among the seven series tested. However, in terms of efficiency, UHP-FRC-T₂-1.5 led to the most cost effective behavior: tensile strength up to $\sigma_{pc} = 14$ MPa, a strain value at peak load $\epsilon_{pc} = 0.60\%$ and a crack spacing $s_{cr} \approx 4$ mm (less than UHP-FRC-H-2.0). This result indicates that optimized composites can be designed with properly manufactured twisted steel fibers (here simply by using a low twist ratio).

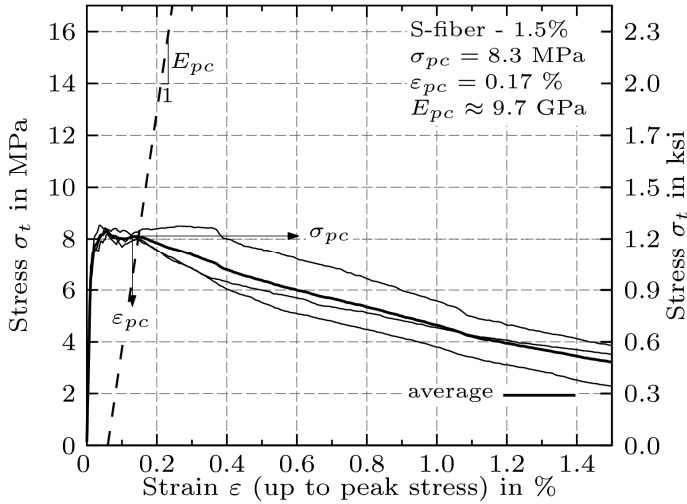


Figure 5. Tensile response of UHP-FRC-S-1.5.

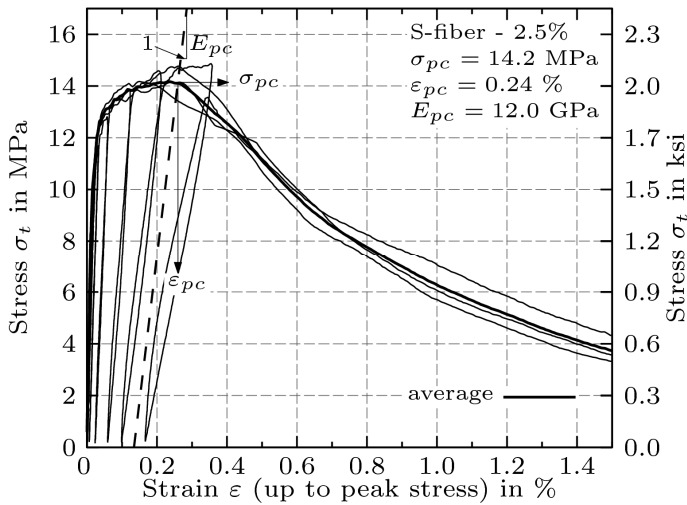


Figure 6. Tensile response of UHP-FRC-S-2.5.

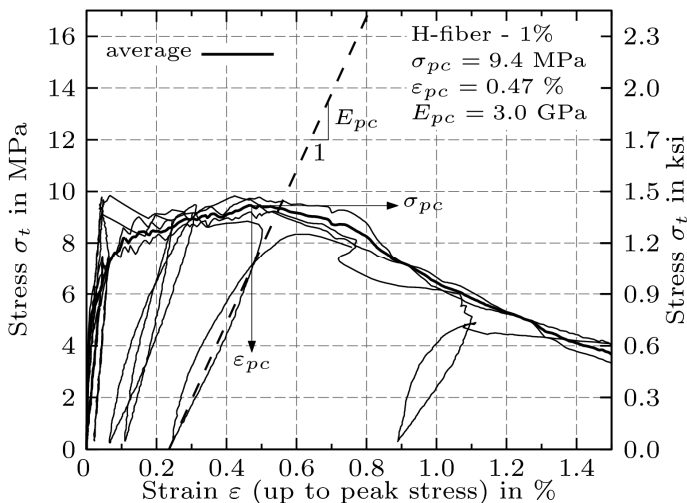


Figure 7. Tensile response of UHP-FRC-H-1.0.

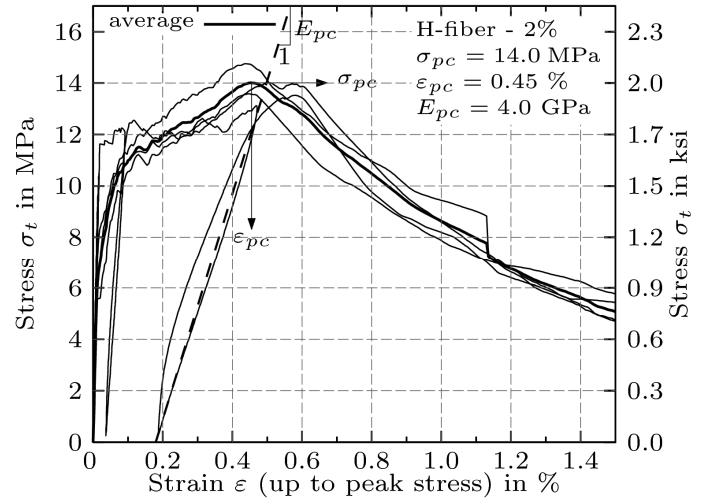


Figure 8. Tensile response of UHP-FRC-H-2.0.

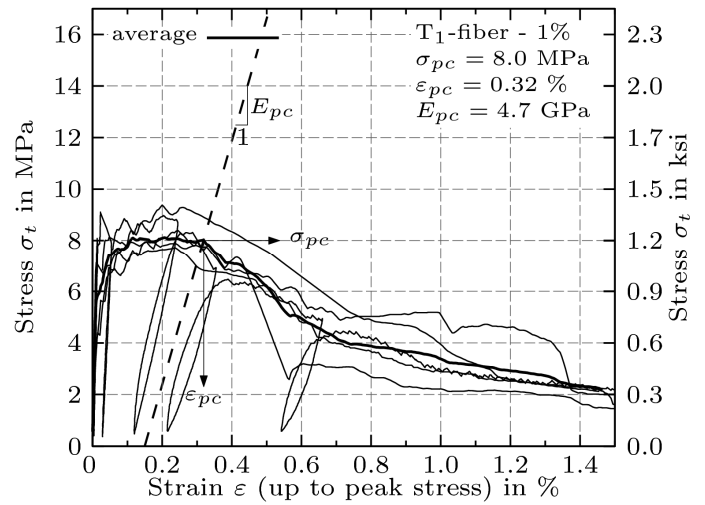


Figure 9. Tensile response of UHP-FRC-T₁-1.0.

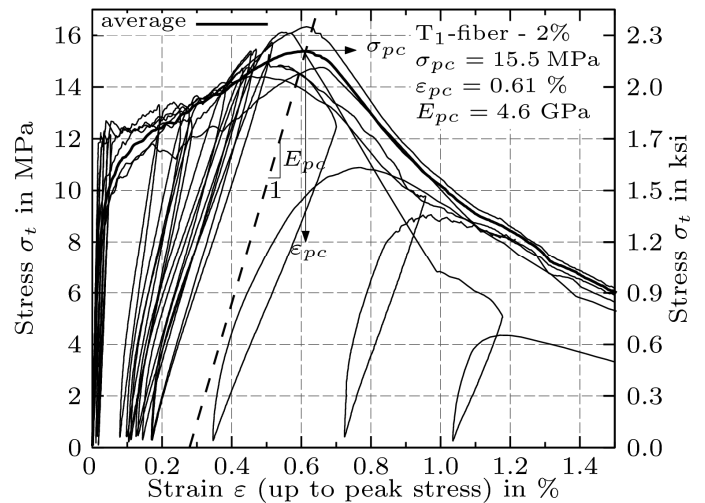


Figure 10. Tensile response of UHP-FRC-T₁-2.0.

Some specimens from each series were loaded and unloaded at different strain levels in order to obtain the unloading stiffness E_u . Surprisingly, all UHP-FRC specimens loaded and unloaded while in the ascending elastic region, eventually exhibited a higher cracking strength than the uniformly loaded specimens.

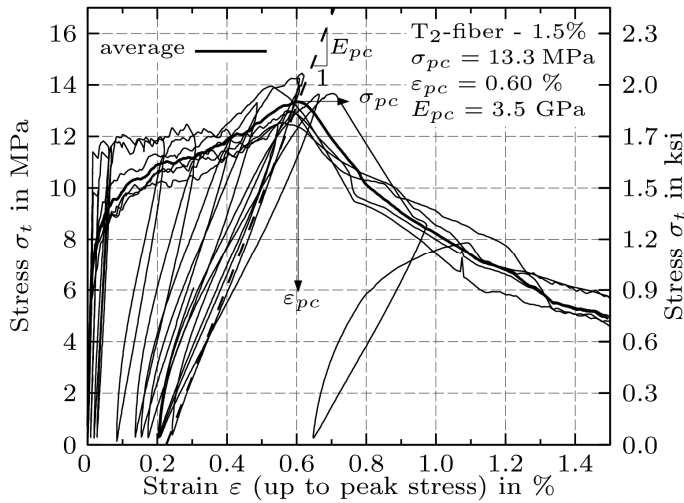


Figure 11. Tensile response of UHP-FRC-T₂-1.5.

Table 4. Average tensile properties of UHPFRCs.

Series	No.	σ_{pc} MPa	ϵ_{pc} %	E_{pc} GPa	n_{cr}	s_{cr} mm
UHP-FRC-S-1.5	3	8.3	0.17	9.7	7	25.4
UHP-FRC-S-2.5	4	14.2	0.24	12.0	22	8.1
UHP-FRC-H-1.0	3	9.4	0.47	3.0	19	9.4
UHP-FRC-H-2.0	5	14.0	0.45	4.0	39	4.6
UHP-FRC-T ₁ -1.0	5	8.0	0.32	4.7	21	8.5
UHP-FRC-T ₁ -2.0	6	15.5	0.61	4.6	58	3.1
UHP-FRC-T ₂ -1.5	6	13.3	0.60	3.5	45	4.0

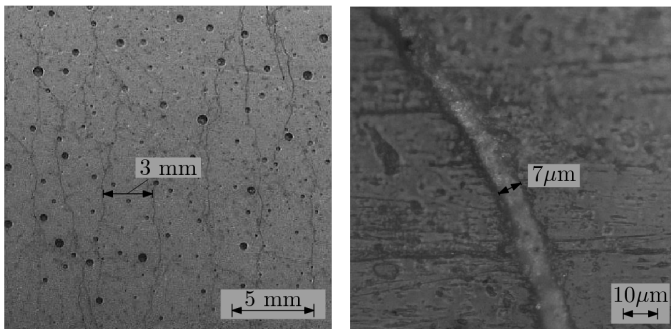


Figure 12. Crack spacing (left) and crack width (right) of UHP-FRC-T₁-2.0.

Experimental values of the unloading stiffness E_u at different strain values within the strain hardening region are plotted in Figure 13 versus the strain at unloading. UHP-FRC including deformed fibers (H & T) follow the same decreasing trend for E_u with increasing strain almost independently of the fiber volume fraction. However, UHP-FRC with S-fibers are significantly stiffer than UHP-FRC-H/T at comparable strain values. This can be explained by the fact that for same volume of fibers, S fibers, having a smaller diameter, offer a much higher surface area for bond and that influences the modulus in the cracked state (Najm & Naaman 1995).

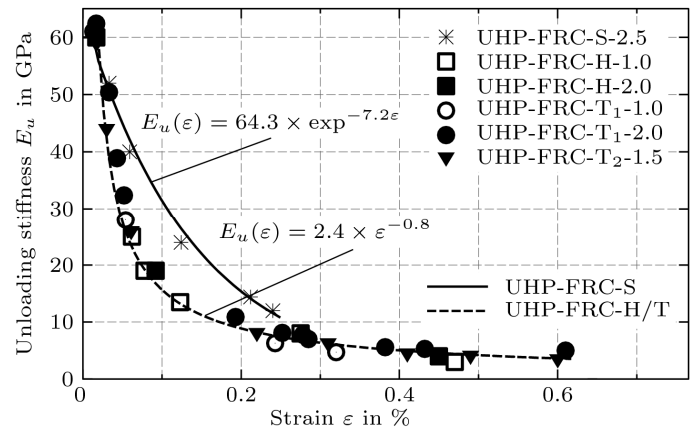


Figure 13. Unloading stiffness E_u of UHPFRCs.

From the values in Table 4 the unloading stiffness at peak load E_{pc} can be fitted, thus calculated, using Equation 8. The factor k_ϵ depends on the type of fiber and was determined to be:

$$\begin{aligned}
 k_\epsilon &= 0.5 && \text{for UHP-FRC with S-fibers} \\
 k_\epsilon &= 0.6 && \text{for UHP-FRC with T-fibers} \\
 k_\epsilon &= 0.7 && \text{for UHP-FRC with H-fibers}
 \end{aligned}$$

5.3 Fracture Energy

The average fracture energy G_f of each test series was calculated using Equations 2-7. This comprises the dissipated energy per unit volume during strain hardening $g_{f,A}$, the dissipated energy per unit ligament area $G_{f,A}$ to open one crack up to δ_{pc} and the dissipated energy per unit ligament area $G_{f,B}$ to completely separate the critical crack during softening. Table 5 and Figure 14-16 summarize the results obtained.

Table 5. Average fracture energy related parameter.

Series	$g_{f,A}$ kJ/m ³	$G_{f,A}$ kJ/m ²	$G_{f,B}$ kJ/m ²	G_f kJ/m ²	δ_{pc} micron
UHP-FRC-S-1.5	9.6	0.24	18.9	19.1	21
UHP-FRC-S-2.5	22.8	0.18	25.1	25.2	10
UHP-FRC-H-1.0	23.7	0.22	21.8	22.1	15
UHP-FRC-H-2.0	28.9	0.13	30.1	30.2	5
UHP-FRC-T ₁ -1.0	16.8	0.14	14.8	14.9	13
UHP-FRC-T ₁ -2.0	54.1	0.17	31.6	31.7	8
UHP-FRC-T ₂ -1.5	37.1	0.15	30.6	30.8	9

Similarly to what was observed for the highest tensile strength and the highest strain value at peak load, UHP-FRC-T₁-2.0 also exhibited the highest fracture energy with $G_f = 32$ kJ/m². This value exceeds 25 kJ/m² reported by Bache (1992) for UHP-FRC using 12 % steel fibers. In terms of efficiency UHP-FRC-T₂-1.5, with 1.5 % fiber content, shows the highest dissipation of energy per unit volume of

fibers, (Fig. 14). The fracture energy of UHP-FRC-S specimens was significantly lower than UHP-FRC-H/T with comparable fiber volume fraction. Nevertheless, UHP-FRC-S-2.5 exhibited 25 kJ/m² in fracture energy, that is about 25 % more than reported by Jungwirth (2006) for a UHP-FRC with same volume fraction of steel fibers.

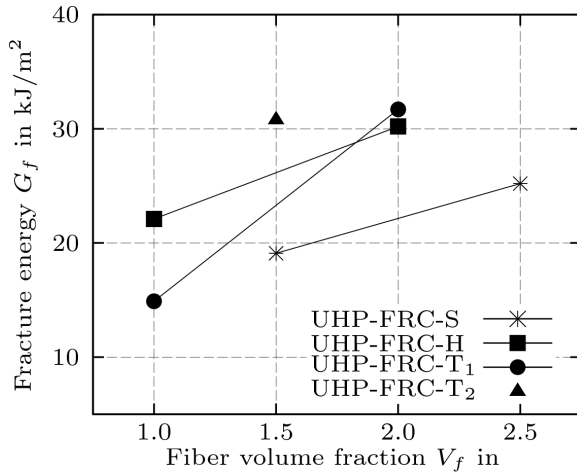


Figure 14. Fracture energy G_f of UHP-FRCs.

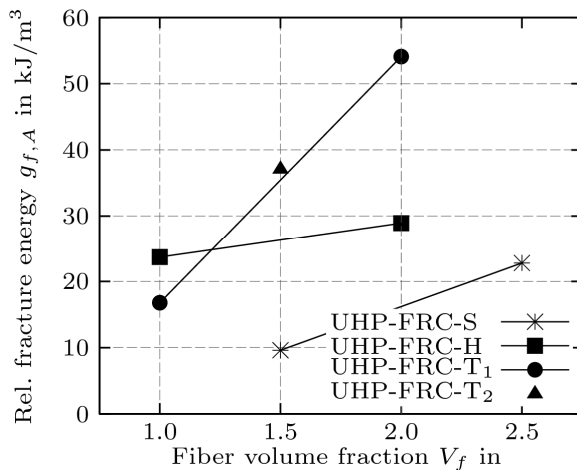


Figure 15. Dissipated energy $g_{f,A}$ per unit volume during strain hardening of UHP-FRCs.

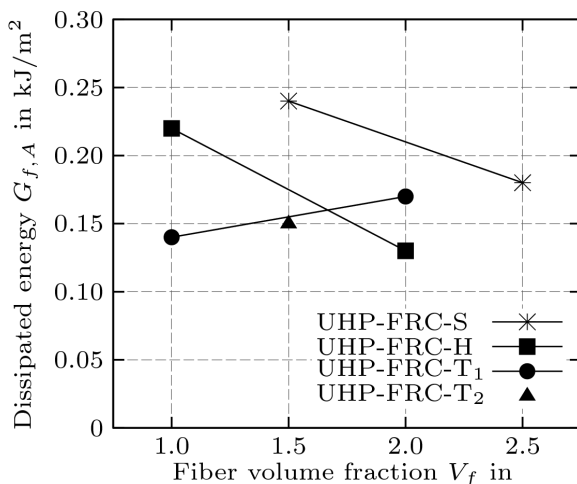


Figure 16. Dissipated energy $G_{f,A}$ per unit ligament area of one crack during strain hardening of UHP-FRCs.

The dissipated energy per unit volume $g_{f,A}$ during strain hardening can be viewed as an evaluation pa-

rameter for the strain hardening performance. Figure 15 illustrate the variation of $g_{f,A}$ in terms of the fiber volume fraction V_f . It can be observed that increasing V_f leads to an increase in $g_{f,A}$. Here again, UHP-FRC-S achieved the lowest values, whereas the highest value of 54 kJ/m³ was attained by UHP-FRC-T₁-2.0.

The dissipated energy per unit ligament area of crack at peak load, $G_{f,A}$, is plotted in Figure 16. With around 0.2 kJ/m² it has only a minor impact on the entire fracture energy. Similar results for $G_{f,A}$ around 0.2 kJ/m² were obtained by Jungwirth (2006).

6 SUMMARY AND CONCLUSIONS

An experimental program with seven series of strain hardening UHP-FRC was carried out to investigate the fracture properties under tensile loading. Special attention was given to clearly distinguish between the energy dissipated during the strain hardening behavior, an energy per unit volume, and the energy needed to completely separate the specimen, an energy per unit surface of crack created. Moreover, the determination of the stiffness at peak load E_{pc} was evaluated in this study.

Through optimization of matrix and fiber parameters, one designed UHP-FRC exhibited a fracture energy $G_f = 32$ kJ/m² with only 2% by volume of high strength twisted steel fibers. This composite achieved a tensile strength in the cracked state, $\sigma_{pc} = 16$ MPa, a strain value at peak load $\varepsilon_{pc} = 0.61\%$, a crack spacing $s_{cr} \approx 3$ mm, and an average residual crack width of 7-8 microns. In terms of efficiency per unit volume of fibers, the highest fracture energy $G_f = 31$ kJ/m² was obtained by using 1.5 % by volume of high strength steel fibers with a low twist ratio. This is about one and a half the fracture energy of comparable UHP-FRC reported by others.

ACKNOWLEDGEMENTS

This work was supported by a fellowship from the Postdoctoral-Programme of the German Academic Exchange Service (DAAD). The second author would like to acknowledge the support of the US National Science Foundation under grant No. CMS 0754505. The authors would also like to acknowledge the following companies for providing free material: Bekaert, Elkem Materials, Grace Construction Products, Lehigh Cement Company. The opinions expressed in this paper are those of the authors and do not necessarily reflect the views of the sponsor.

REFERENCES

Bache, N. H. 1992. Principles of similitude in design of rein-

- forced brittle matrix composites. in H. W. Reinhardt & A. E. Naaman (eds). 1992. *High Performance Fiber Reinforced Cement Composites*. Rilem Proceedings 15, Published by E & FN Spon. London. 1992. pp. 39 – 56.
- Benson, S. D. P. & Karihaloo, B. L. 2005. CARDIFRC – Development and mechanical properties. Part III: Uniaxial tensile response and other mechanical properties. *Magazine of Concrete Research*. Vol. 57. No. 8. pp. 433 – 443.
- Habel, K., Viviani, M., Denarie, E. & Bruehwiler, E. 2006. Development of the mechanical properties of an Ultra-High Performance Fiber Reinforced Concrete (UHPFRC). *Cement and Concrete Research*. No. 36. pp. 1362 – 1370.
- Jungwirth, J. 2006. Zum Tragverhalten von zugbeanspruchten Bauteilen aus Ultra-Hochleistungs-Faserbeton. Ecole Polytechnique Federale de Lausanne. Ph.D. thesis.
- Maalej, M., Hashida, T. & Li, V. C. 1995. Effect of Fiber Volume Fraction on the Off-Crack-Plane Fracture Energy in Strain-Hardening Engineering Cementitious Composites. *Journal of the American Ceramic Society*. Vol. 78. No. 12. pp. 3369 – 3375.
- Markovic, I. 2006. High-Performance Hybrid-Fibre Concrete – Development and Utilisation. Delft University. Ph.D. thesis.
- Naaman, A.E., 2007 Tensile Strain-Hardening FRC Composites: Historical Evolution since the 1960's, in proceedings of International Workshop on Advanced Construction Materials, C.U. Gross, Editor, Springer-Verlag Berlin Heidelberg, pp. 181-202.
- Najm, H., and Naaman, A.E., 1995 Prediction Model for the Elastic Modulus of High Performance Fiber Reinforced Cement Based Composites, *ACI Materials Journal*, Vol. 92, No. 3, pp. 304-314.
- Richard, P. & Cheyrezy, M. 1995. Composition of reactive powder concretes. *Cement and Concrete Research*. Vol. 25. No. 7. pp. 1501 – 1511.
- Wille, K., Naaman, A. E. & Parra-Montesinos, G. J. 2009. Ultra high performance concrete with compressive strength exceeding 150 MPa (22 ksi): The simpler way. *ACI Materials Journal*. submitted.